ISSN 1061-933X, Colloid Journal, 2021, Vol. 83, No. 6, pp. 787–793. © Pleiades Publishing, Ltd., 2021.

Microwave Synthesis of Fe_3O_4/Poly(styrene-*co*-acrylic acid) Microspheres with a Narrow Size Distribution

Junjun Tan[a], *, Yanxiang Li[b], **, and Yimin Sun[a]

[a] *College of Chemistry and Materials Science, Anhui Normal University, Wuhu, 241002 China*

[b] *Key Laboratory of Green Process and Engineering, Institute of Process Engineering, Chinese Academy of Sciences, Beijing, 100190 China*

**e-mail: tjj@iccas.ac.cn*

***e-mail: yxli@ipe.ac.cn*

Received November 14, 2020; revised June 23, 2021; accepted July 11, 2021

Abstract—Magnetite microspheres have wide applications in industry and biomedicine. The control of the particle size and size distribution is critical in accurately controlling the chemical and physical properties of the magnetic nanoparticles. Here an efficient microwave-controlled synthesis of Fe_3O_4/P(St-AA) microspheres was reported. We found that the reaction rate was accelerated and the size distribution was narrowed with the microwave-assisted synthesis. The size of the microspheres can be controlled by the feeding concentration of the sodium dodecyl benzene sulfonate surfactant with diameters ranging from 200~400 nm. Meanwhile, the magnetic microspheres exhibit superparamagnetic properties with no hysteresis at the low applied magnetic field, which is important for their application in magnetic field-driven applications.

DOI: 10.1134/S1061933X21060156

INTRODUCTION

Magnetite (Fe_3O_4) nanoparticles exhibit superparamagnetism and quantum tunneling of magnetization by uniquely combining mesoscale and magnetic properties [1]. The easy preparation, biocompatibility, and non-toxicity further confer them plenty of applications in biomedicine, biotechnology, and industry, such as magnetic resonance imaging (as contrast agents), hyperthermia treatment, cell sorting, magnetically targeted drug delivery, analytic sensing, separation, conversion of CO_2, etc. [2–9]. However, the surface uncoated Fe(II) cations are susceptible to oxidation to form a shell of γ-Fe_2O_3 and cause the nanoparticles to aggregate. The encapsulation of the nanoparticles with organic shells can stabilize the nanoparticles and introduce functional groups to exert diverse functions. The encapsulation methods include direct surface modification with small organic molecules and polymers, in situ nanoparticle synthesis, and direct surface polymerization to meet different functionalization requirements for their applications [3, 9–16].

Besides the introduction of diverse functional groups, particle size and size distribution also affect both the physical and chemical properties of the nanoparticles and nanocomposites [17, 18]. The control of the particle size and size distribution is critical in accurately controlling and differentiate their properties for further applications [17–19].

However, it is still challenging to synthesize Fe_3O_4 nanoparticles with a narrow size distribution. Several polymerization methods have been explored to prepare the nanoparticles such as dispersion polymerization, emulsion polymerization, and miniemulsion polymerization [3, 11, 15, 16]. The polymerization conditions such as solvent ratio, temperature, the concentration of monomer, initiator, and surfactant, etc. can be used to control the particle size and distribution, but the reported examples have not provided ideal narrow size distribution so far.

Microwave energy has long been used for the synthesis of both nanoparticles and organic synthesis [20]. Microwave-assisted heating has been proven to be environmentally benign and very efficient because microwave energy can selectively heat the reactants, accelerate reaction rate, reduce side reactions, increase reaction yield, and in some cases lead to homogeneous nucleation and give rise to relatively uniform inorganic or organic nanoparticles [20–23]. It was also proved very efficient in synthesizing Fe_3O_4 nanoparticles [24, 25]. Moreover, in emulsion polymerization, microwave-assisted heating accelerates the reaction and greatly narrows the size distribution of the resulting latexes [22, 23]. Thus we posit that the

emulsion polymerization on the nanoparticle surface should also give rise to inorganic/organic microspheres with the narrow size distribution.

We thus propose the microwave-assisted heating method to prepare both Fe_3O_4 nanoparticles and Fe_3O_4/polymer microspheres to improve the preparation process and narrow the size distribution of the nanocomposite particles. An improved microwave-assisted co-precipitation method was used to facilitate the synthesis of the Fe_3O_4 nanoparticles at the first step. Then we selected the classical polymerization monomer styrene (St) and a small amount of acrylic acid (AA) to copolymerize on their surface to obtain the core-shell structured Fe_3O_4/P(St-AA) microspheres. Introducing AA cannot only improve the hydrophilicity of the composite microspheres but also introduce functional carboxylic groups for future applications. The magnetic properties of the resulting nanoparticles were further investigated.

MATERIALS AND METHODS

Reagents and Instruments

$FeSO_4 \cdot 6H_2O$, $FeCl_3 \cdot 7H_2O$, and NaOH (Chinese Medical Chemical Reagent Co., Shanghai, China) were used directly without further treatment. Styrene (St) and Acrylic acid (AA) (Chinese Medical Chemical Reagent Company, Shanghai, China) were distilled under reduced pressure before use. Potassium persulfate (KPS) (Shanghai Aijian Chemical Reagent Co.) was recrystallized and dried before use. Ethanol (≥99.5%, analytical grade) (Shanghai Zhenxing Chemical Plant) and sodium dodecyl benzene sulfonate (SDBS) (Shanghai Chemical Reagent Co., China) were used directly without any further purification.

A microwave oven was equipped with a flask, a mechanical stirrer, a reflux condenser, and feeding heads assembled inside the oven, operating at 2450 MHz with a maximum output power of 800 W.

Synthesis of Fe_3O_4 Nanoparticles and Fe_3O_4/P(St-AA) Nanocomposites

The Fe_3O_4 nanoparticles were prepared with a microwave-assisted co-precipitation method according to the following reaction.

$$2Fe^{3+} + Fe^{2+} + 8OH^- \rightarrow Fe_3O_4 + 4H_2O.$$

An aqueous solution of $FeCl_3$ (2.0 mol/L, 10 mL), $FeSO_4$ (1.0 mol/L, 12 mL), and water (18 mL) were mixed together by vigorous stirring in a conical flask. $FeSO_4$ was in excess relative to the reaction stoichiometry. NaOH (9 mol/L, 10 mL) was added to the mixture and the solution was strongly stirred for 5 min. The flask was then transferred into a microwave reactor to react for 2 min under maximum power output to produce the Fe_3O_4 nanoparticle dispersion. After cooling down, the as-prepared Fe_3O_4 nanoparticles were washed with distilled water several times by magnet attraction and dispersion until the pH reached 9~10 to keep them in a well-dispersed state, and Fe_3O_4 content was adjusted to be around 5%. Finally, the resulted ferrofluid was purged with nitrogen and reserved in the refrigerator for further reaction later.

100 mL of 20% ethanol/water mixture (v/v), ferrofluid (5 mL, 5%), KPS (3 mL, 0.05mol/L), and a certain amount of SDBS were added into a three-necked flask, stirred, and sonicated for 5 min. Then St (3 mL) and AA (0.5 mL) were added and sonicated again for 5 min. The flask was then transferred to the microwave reactor equipped with a water-cooled condenser, thermometer, and N_2 inlet. The reaction mixture was stirred under a N_2 atmosphere for 30 min and then heated for several minutes with 800 W microwave irradiation until the temperature reached 80°C. This temperature was maintained with a microwave irradiation of 110 W for 6 h and the flask was then cooled to room temperature. For comparison, the same reaction was conducted at 80°C with traditional heating in an oil bath. Thereafter, the obtained magnetic microspheres were collected by imposing a magnetic field and washed with water several times. The products were then dried in a vacuum oven at 30°C for 24 h.

Characterization

All transmission electron microscopy (TEM) was done using a Hitachi H-600 microscope operating at 75 kV. To prepare the TEM samples, 10 μL of well-dispersed sample solutions were dropped onto the TEM copper grids (Electron Microscopy Sciences, USA) for 1 min before the excess solution was wicked by the filter paper. Image J software was used to measure the average particle size and determine the standard deviation from the collected TEM images.

Fourier transform infrared (FT-IR) spectra of the Fe_3O_4 nanoparticles and Fe_3O_4/P(St-AA) microspheres were acquired on a Bruker Tensor 27 FT-IR spectrometer with KBr pellet method.

Thermal gravimetric analysis (TGA) of the particles was performed using DT-40 Thermal Analyzer (Japan). The TGA measurements were carried out with a heating rate of 10°C/min under nitrogen atmosphere with α-Al_2O_3 as reference.

The X-ray diffraction (XRD) was carried out on a Japan Rigaku D/max-rA rotation anode X-ray diffractometer to characterize the microstructures and phases of the nanoparticles.

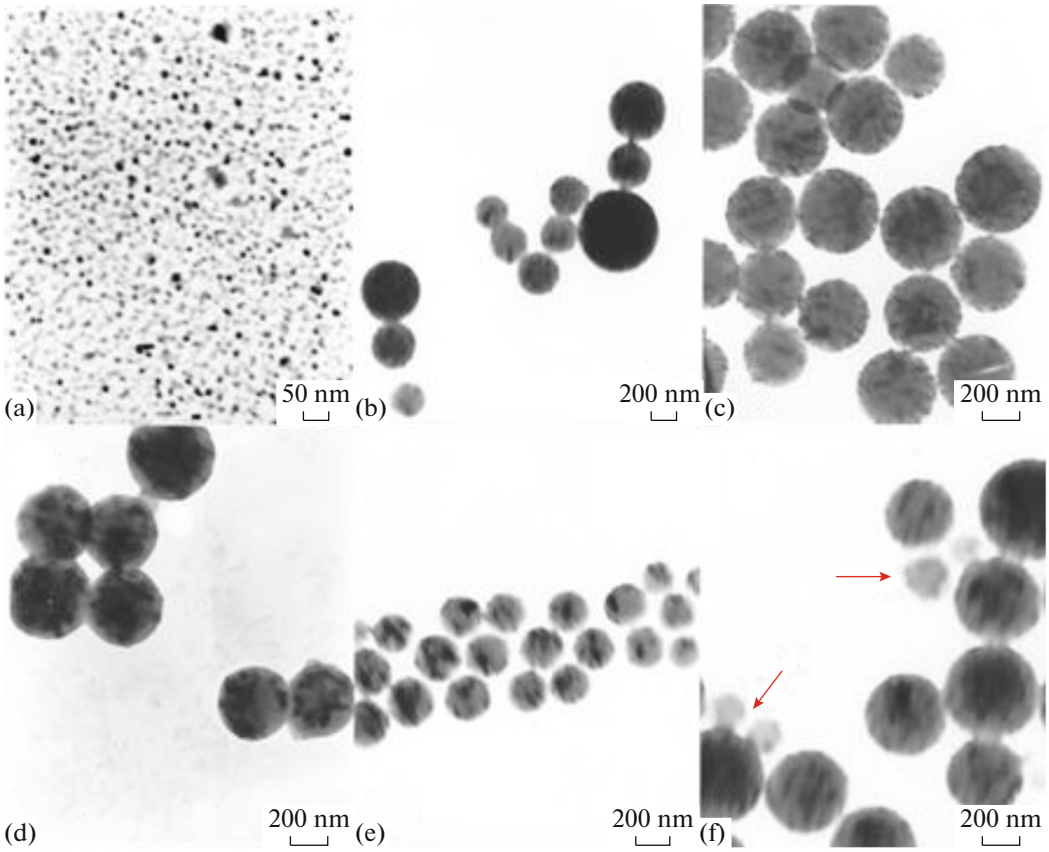

Fig. 1. TEM images of Fe_3O_4 nanoparticles (a), Fe_3O_4/P(St-AA) microspheres from samples O-1 (b), M-1 (c), M-2 (d), M-3 (e), and the crude dispersion of M-1 (f). The red arrows in (F) show relatively smaller polymeric microspheres without Fe_3O_4 nanoparticles.

The magnetic properties of the microspheres were characterized with a Lakeshore 7307 vibrating-sample magnetometer under a magnetic field up to 10 kOe at room temperature.

RESULTS AND DISCUSSION

Microwave-assisted heating was proved very efficient in synthesizing Fe_3O_4 nanoparticles [24, 25]. The synthetic process usually takes less than 30 min. Here, we improved and simplified the microwave-assisted synthesis of Fe_3O_4 nanoparticles by using the classic co-precipitation method as described in the experimental part. The ferrofluid is formed within 2 min, which greatly simplifies the preparation process and shortens the reaction time. The TEM image (Fig. 1a) indicates that the Fe_3O_4 nanoparticles have an average diameter of 12 ± 2 nm.

The XRD patterns of the as-prepared nanoparticles (Fig. 2a) confirm the face-centered cubic Fe_3O_4 phase according to the Joint Committee on Powder Diffraction Standards (JCPDS card 19-629). FT-IR proves the formation of Fe_3O_4 with the presence of Fe–O vibration at 584 cm^{-1} (Fig. 2b).

A series of Fe_3O_4/P(St-AA) microspheres was prepared under different reaction conditions, as shown in Table 1. O-1 and M-1 samples were synthesized according to the same protocol but using different heating sources (thermal heating and microwave heat-

Table 1. Conditions for the synthesis of Fe_3O_4/P(St-AA) microspheres and their diameters

Sample	Heating method	Reaction time, h	[SDBS], mol/L	Average diameter, nm
O-1	Oil bath	24	1.2×10^{-3}	375 ± 116
M-1	Microwave	6	1.2×10^{-3}	403 ± 28
M-2	Microwave	6	2.5×10^{-3}	398 ± 22
M-3	Microwave	6	3.4×10^{-3}	247 ± 18

The composition of the reaction mixture: 5 mL ferrofluid, 3 mL St, 0.5 mL AA, and 1.5 mM KPS in 100 mL 20% (v/v) ethanol/water solution.

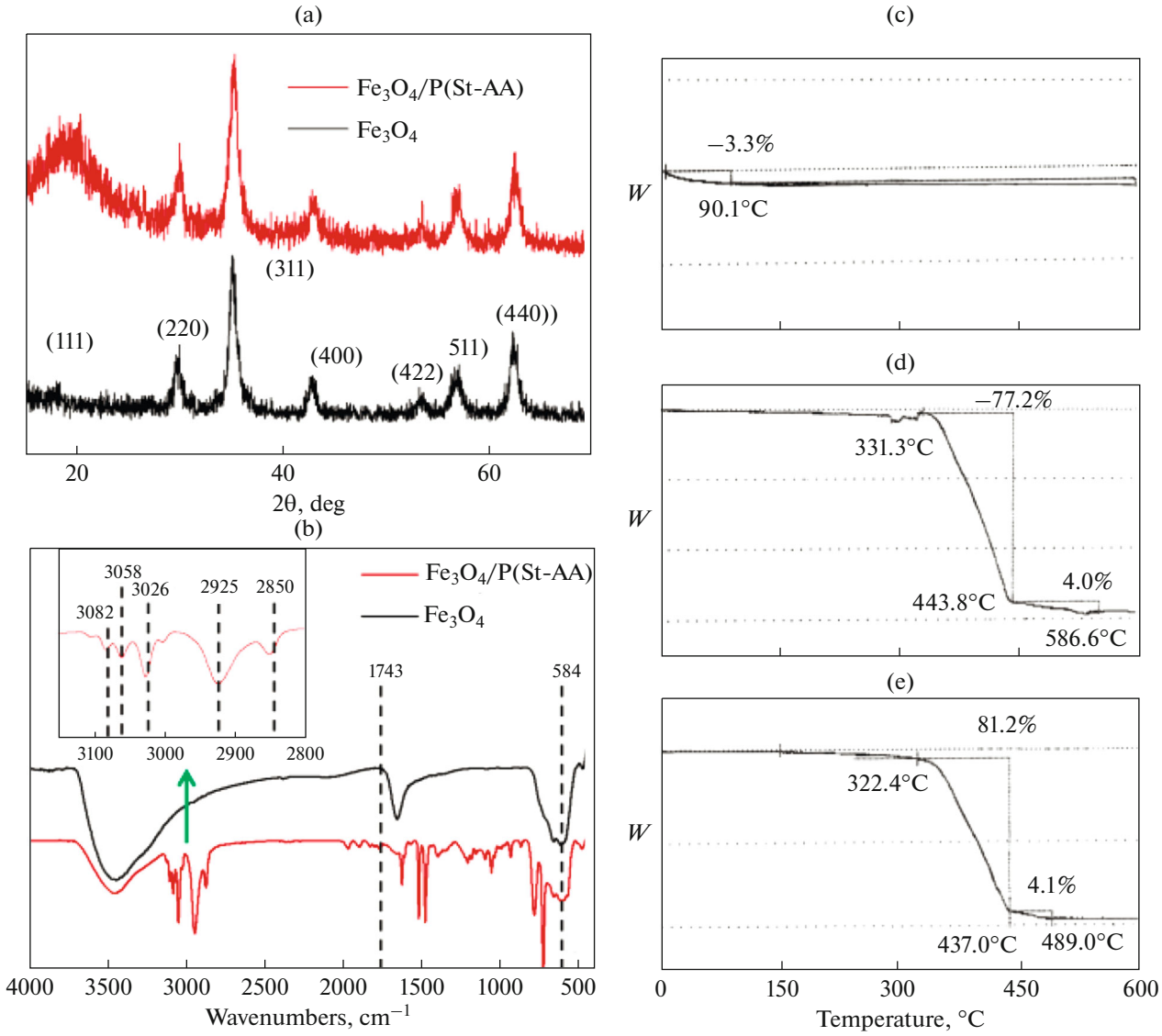

Fig. 2. XRD (a) and FT-IR (b) data for Fe_3O_4 and Fe_3O_4/P(St-AA) particles and TG curves of Fe_3O_4 nanoparticles (c) and Fe_3O_4/P(St-AA) microspheres from samples M-1 (d) and M-3 (e).

ing, respectively). As for M-1, M-2, M-3 samples, the reactions were carried out under microwave irradiation with various concentrations of SDBS.

The TEM images indicate all the microspheres were composed of many small Fe_3O_4 nanoparticles (Fig. 1). For comparison, when synthesizing sample O-1, the reaction was carried out for 6, 12, and 24 h, and it was found that the reaction was complete after 24 h under oil bath heating which is consistent with the literature report [3]. The TEM image of the resulting microspheres is shown in Fig. 1b. We can see the microspheres are quite different in size. However, under microwave irradiation, well-defined and uniform microspheres (Figs. 1c–1e) were formed just in 6 h in the case of M-1, M-2, and M-3 samples, which means the irradiation accelerate the polymerization and narrows down the size distribution of the microspheres greatly.

The size distribution of sample O-1 prepared under thermal heating is 375 ± 116 nm, while the size distributions of samples M-1, M-2, and M-3 synthesized under microwave heating are 403 ± 28, 398 ± 22, and 247 ± 18 nm, respectively (Table 1). Moreover, the average size of the microspheres can be easily controlled by changing the concentration of SDBS. Increasing the concentration of SDBS can decrease the diameter from 403 ± 28 to 247 ± 18 nm as higher SDBS concentration can give rise to more micelles

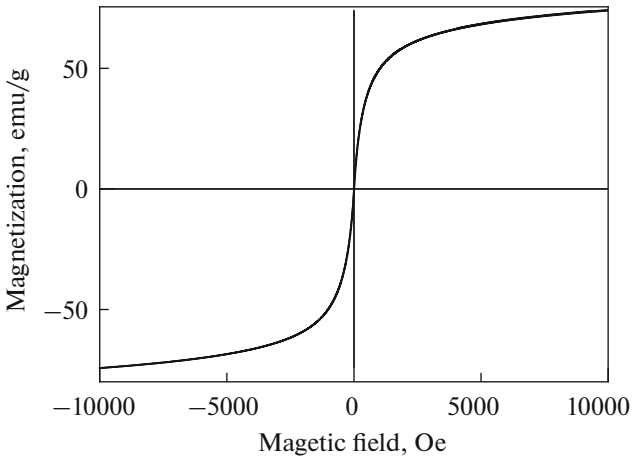

Fig. 3. The magnetization loop of the sample M-1.

with less monomer for polymerization in each micelle. It is reported that the ratio of monomers to the magnetic fluid affects the average size of the resulting microspheres [26], while here we present an alternative approach to control the average size of composite microspheres.

The XRD pattern of the Fe_3O_4/P(St-AA) microspheres has a reflection characteristic of amorphous polymer in addition to the Fe_3O_4 reflections (Fig. 2a). From Fig. 2b, besides the Fe–O vibration at 584 cm^{-1}, the IR spectrum of the microspheres showed C–H stretching vibrations of aromatics (at 3082, 3058, 3032 cm^{-1}) and the methylene asymmetric and symmetric stretching vibrations at 2925 and 2850 cm^{-1}, respectively. The band at 1743 cm^{-1} was attributed to the C=O stretching vibration of the carboxyl group. As the monomer AA was added in a small ratio to St in the polymerization, the band corresponding to the carboxyl group is relatively weak. All these prove that the organic shell of the microspheres are composed of the copolymer P(St-AA).

TGA data for the Fe_3O_4 nanoparticles and Fe_3O_4/P(St-AA) microspheres of samples M-1 and M-3 are shown in Figs. 2c, 2d, 2e, respectively. The TGA curve of the Fe_3O_4 nanoparticles shows only small weight loss around 3.3% due to moisture evaporation (Fig. 2c). And curves for the Fe_3O_4/P(St-AA) microspheres show a gradual weight loss with the increase of temperature. Except for the slight evaporation of water, the gradual weight loss is attributed to the decomposition of the P(St-AA) (Figs. 2d, 2e). Only the inorganic Fe_3O_4 is left, and the weight loss indicates the Fe_3O_4 content is around 18.8 wt % for the microspheres of sample M-1 (Fig. 2d) and 14.7 wt % for sample M-3 (Fig. 2e), respectively, which means the higher SDBS concentration in the reaction can give rise to a lower Fe_3O_4 content and higher polymer portion in the microspheres because higher SDBS concentration gives rise to more micelles with less Fe_3O_4 for the surface polymerization.

We further characterized the magnetic properties of the composite microspheres. These magnetic microspheres exhibit superparamagnetic behavior at 300 K with a high saturation magnetization of 74 emu/g and without hysteresis at a low applied mag-

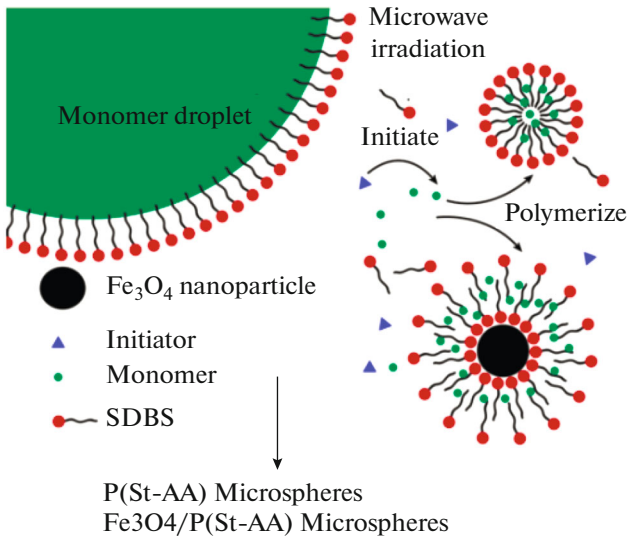

Fig. 4. Schematic presentation of emulsion polymerization in the presence of Fe_3O_4 nanoparticles.

netic field, which is very important for magnetic field-driven applications (Fig. 3).

The mechanism of the emulsion polymerization in the presence of inorganic nanoparticles was further explored. As the surface of the Fe_3O_4 nanoparticles is hydrophilic, SDBS surfactant would be adsorbed and form bilayers on the surface of the Fe_3O_4 nanoparticles to give rise to Fe_3O_4/SDBS micelles, as reported in the literature [13]. As St is in a much higher ratio, the micelles will allow the initiation and further polymerization of the St monomers and copolymerization with the AA to form the core-shell microspheres with P(St-AA) as shell and Fe_3O_4 as core inside (Fig. 4). Thus, with the increase of SDBS concentration, the number of micelles increases while the size of microspheres and the Fe_3O_4 content decrease. As the TEM results indicate that the microspheres are composed of many Fe_3O_4 nanoparticles, we inferred that the Fe_3O_4-containing micelles aggregate during the polymerization gave rise to these big microspheres with a number of Fe_3O_4 small nanoparticles inside. SDBS molecules can also form a small amount of micelles themselves for emulsion polymerization without Fe_3O_4 nanoparticles (Fig. 4), which is proved by the presence in the TEM image of a few small latex particles without Fe_3O_4 inside (noted with red arrows in Fig. 1f) in the crude reaction dispersion before its purification and separation.

CONCLUSION

Microwave irradiation can induce rotation of the dipoles within the liquid, force the water to align and relax in the field of oscillating electromagnetic radiation, and uniformly heat up the entire solution to prepare narrowly distributed latex particles in emulsion polymerization as the polymerization could be simultaneously initiated and the rate of the initiation should be a constant [22, 23]. Here we shown that microwave heating can even give rise to a narrow distribution of the Fe_3O_4/P(St-AA) microspheres with shorter reaction time than thermal heating. The size of the microspheres can be controlled by adjusting the concentration of SDBS. The efficient synthetic method would be perspective in preparing all kinds of functional microspheres with narrow distribution and for future industrial and biomedical applications.

ACKNOWLEDGMENTS

This work was supported by the National Nature Science Foundation of China (Grant no. 21978307).

CONFLICT OF INTEREST

There are no conflicts to declare.

REFERENCES

1. Laurent, S., Forge, D., Port, M., Roch, A., Robic, C., Van der Elst, L., and Muller, R.N., *Chem. Rev.,* 2008, vol. 108, no. 6, pp. 2064–2110.
2. Xuan, S., Wang, F., Lai, J.M.Y., Sham, K.W.Y., Wang, Y.-X.J., Lee, S.-F., Yu, J.C., Cheng, C.H.K., and Leung, K.C.-F., *ACS Appl. Mater. Interfaces,* 2011, vol. 3, no. 2, pp. 237–244.
3. Chen, Z., Liu, L., Wu, X., and Yang, R., *RSC Adv.,* 2016, vol. 6, no. 110, p. 108583–18589.
4. Gupta, A.K. and Gupta, M., *Biomaterials,* 2005, vol. 26, no. 18, pp. 3995–4021.
5. Urbanova, V., Magro, M., Gedanken, A., Baratella, D., Vianello, F., and Zboril, R., *Chem. Mater.,* 2014, vol. 26, no. 23, pp. 6653–6673.
6. Shao, M., Ning, F., Zhao, J., Wei, M., Evans, D.G., and Duan, X., *J. Am. Chem. Soc.,* 2012, vol. 134, no. 2, pp. 1071–1077.
7. Zhuang, F., Tan, R., Shen, W., Zhang, X., Xu, W., and Song, W., *J. Alloys Compd.,* 2015, vol. 637, pp. 531–537.
8. Jiang, J., Wen, C., Tian, Z., Wang, Y., Zhai, Y., Chen, L., Li, Y., Liu, Q., Wang, C., and Ma, L., *Ind. Eng. Chem. Res.,* 2020, vol. 59, no. 5, pp. 2155–2162.
9. Shultz, M.D., Calvin, S., Fatouros, P.P., Morrison, S.A., and Carpenter, E.E., *J. Magn. Magn. Mater.,* 2007, vol. 311, no.1, pp. 464–468.
10. Cui, L., Gu, H., Xu, H., and Shi, D., *Mater. Lett.,* 2006, vol. 60, no.24, pp. 2929–2932.
11. Sun, Y., Wang, B., Wang, H., and Jiang, J., *J. Colloid Interface Sci.,* 2007, vol. 308, no. 2, pp. 332–336.
12. Wang, L., Housel, L.M., Bock, D.C., Abraham, A., Dunkin, M.R., McCarthy, A.H., Wu, Q., Kiss, A., Thieme, J., Takeuchi, E.S., Marschilok, A.C., and Takeuchi, K.J., *ACS Appl. Mater. Interfaces,* 2019, vol. 11, no. 22, pp. 19920–19932.
13. Lee, H.-H., Yamaoka, S., Murayama, N., and Shibata, J., *Mater. Lett.,* 2007, vol. 61, no. 18, pp. 3974–3977.
14. Berry, C.C., Wells, S., Charles, S., and Curtis, A.S.G., *Biomaterials,* 2003, vol. 24, no. 25, pp. 4551–4557.
15. Guo, L., Pei, G.-L., Wang, T.-J., Wang, Z.-W., and Jin, Y., *Colloids Surf., A,* 2007, vol. 293, nos. 1–3, pp. 58–62.
16. Yanase, N., Noguchi, H., Asakura, H., and Suzuta, T., *J. Appl. Polym. Sci.*, 1993, vol. 50, no. 5, pp. 765–776.
17. Maaz, K., Karim, S., and Kim, G.-H., *Chem. Phys. Lett.,* 2012, vol. 549, pp. 67–71.
18. Motoyama, J., Hakata, T., Kato, R., Yamashita, N., Morino, T., Kobayashi, T., and Honda, H., *Biomagn. Res. Technol.,* 2008, vol. 6, p. 4.
19. Beveridge, J.S., Stephens, J.R., and Williams, M.E., *Annu. Rev. Anal. Chem.,* 2011, vol. 4, pp. 251–273.

20. Galema, S.A., *Chem. Soc. Rev.,* 1997, vol. 26, no. 3, pp. 233–238.

21. Zhu, Y.-J. and Chen, F., *Chem. Rev.,* 2014, vol. 114, no. 12, pp. 6462–6555.

22. Murray, M., Charlesworth, D., Swires, L., Riby, P., Cook, J., Chowdhry, B.Z., and Snowden, M.J., *J. Chem. Soc., Faraday Trans.,* 1994, vol. 90, no. 13, pp. 1999–2000.

23. Zhang, W., Gao, J., and Wu, C., *Macromolecules,* 1997, vol. 30, no. 20, pp. 6388–6390.

24. Jaiswal, K.K., Manikandan, D., Murugan, R., and Ramaswamy, A.P., *Eur. Polym. J.,* 2018, vol. 98, pp. 177–190.

25. Williams, M.J., Sanchez, E., Aluri, E.R., Douglas, F.J., MacLaren, D.A., Collins, O.M., Cussen, E.J., Budge, J.D., Sanders, L.C., Michaelis, M., Smales, C.M., Cinatl, J.J., Lorrio, S., Krueger, D., de Rosales, R.T.M., and Corr, S.A. *RSC Adv.,* 2016, vol. 6, no. 87, pp. 83520–83528.

26. Huang, J., Pen, H., Xu, Z., and Yi, C., *React. Funct. Polym.,* 2008, vol. 68, no. 1, pp. 332–339.